

# The influence of magnetic reversed shear in the improvement of quality of confinement in the plasma of Tokamak: Comparison between TEXTOR & ITER

M. El Mouden<sup>1</sup>, A. Dezairi<sup>2</sup>, D. Saifaoui<sup>1</sup>, B. Zine<sup>1</sup>, M. Eddahby<sup>2</sup>, A. Rouak<sup>1</sup>

1. *Laboratory of theoretical and Applied Physics, Faculty of Sciences- Ain Chock, Casablanca, Morocco,*

2. *Laboratory of the Physics of Condensed Matter, Faculty of Sciences- Ben M'sik, Casablanca, Morocco,*

The reversed magnetic shear is the most important factor in the studies of the plasmas of tokamak. In this paper we focus our research, at first stage, on the control of the improved confinement regimes by studying the influence of reversed shear on its quality in the plasma of tokamak and especially in reducing the anomalous transport in TEXT and ITER, then we study the influence of perturbation's modes in the particles diffusion. In the whole simulations, a comparison between results obtained using ITER and TEXT parameters is carried out.

**Key words:** Plasma confinement, Tokamak, Anomalous transport, Magnetic shear, Transport barrier, Particles diffusion and radial electric field.

## I-INTRODUCTION

Confinement of thermonuclear plasma in tokamak toroidal magnetic containers is a highly promising approach to the realisation of fusion reactors for central station electrical generating plants. Important new results obtained in experiments, theory and modelling enable an improved understanding of the physical processes occurring in tokamak plasmas and give enhanced confidence to achieve tokamak's goals. In particular, progress has been demonstrated by the increase of the triple product  $nT\tau$  (Lawson Criteria) by about four orders of magnitude. Now ITER is near of the ignition phases which characterise the industrial uses of energy produced by tokamaks.

The pathway to plasma regimes with reduced transport and improved confinement has been greatly advanced by understanding the important role of the radial electric field  $E_r$  in the formation of transport barriers in tokamak plasmas. More specifically, the transport reduction results from the nonlinear decorrelation and linear stabilization of turbulent eddy by the  $E \times B$  velocity shear.

In this paper, we compare the entire mapping results<sup>1, 8-17</sup> obtained using tow tokamaks: TEXTOR and ITER, and how can that contribute to the improvement of confinement in tokamak especially in the configuration known as of reversed magnetic shear which is more adopted in the new machines of fusion, since we observe important reductions there in the diffusion coefficient. This result is carried out in the next sections.

## II – MAPPING EQUATIONS<sup>1, 8-17</sup>:

**I-1 Equation of motion:** In our survey, we use a simplified model of an equilibrium magnetic field, according to toroidal geometry, which is described by the following relation:

$$\vec{B} = B\theta(r)\vec{e}_\theta + B\varphi\vec{e}_\varphi \quad (1)$$

consists of the poloidal magnetic field component and the toroidal magnetic field component

which are bound through the relation:

$$B\theta(r) = \frac{r}{q(r)R_0} B\varphi, \text{ of which } r \text{ is the minor radius}$$

of plasma,  $\theta$  and  $\varphi$  are respectively the poloidal and toroidal angle, and finally,  $q(r)$  is the safety factor.

In the Gauss units system, the equation of the motion of the guiding center is given by:

$$\frac{d\vec{x}}{dt} = v_{||} \frac{\vec{B}}{\|\vec{B}\|} + c \frac{\vec{E} \wedge \vec{B}}{B^2} \quad (2)$$

where,  $v_{||}$  is the parallel velocity,  $\vec{E}$  and  $\vec{B}$  are the electric and magnetic fields, and the last term of this equation represents the drift velocity.

The electric field satisfies the relation:

$$\vec{E} = -\vec{\nabla}\phi \quad (3)$$

The correspondent electrostatic potential  $\phi$  can be written as the sum of two terms, the first is the radial part supposed at equilibrium, and the second one

represents the fluctuating part, noted  $\tilde{\phi}$ . We use the model of the spectrum of drift wave, and we have:

$$\tilde{\phi} = \sum_{m,l,n} \phi_{m,l,n} \cos(m\theta - l\varphi - n\omega_0 t) \quad (4)$$

where,  $\omega_0$  is the lowest angular frequency in the spectrum of drift wave, and  $\theta$  and  $\varphi$  are random variables.

The disrupted electrostatic field  $\tilde{E}$  is joined to the potential of perturbation with<sup>1</sup>:

$$\tilde{E} = -\vec{\nabla} \tilde{\phi}.$$

In the continuation of our survey, we suppose that  $B \approx B_\phi \gg B_\theta$  and  $B_r = 0$  respect the

system of toroidal coordinates  $(r, \theta, \varphi)$  and we introduce  $\bar{E}_r$  as the equilibrium radial electric field. The previous equation of motion will be projected in this system of coordinates, and we get the following system:

$$\begin{aligned} \frac{dr}{dt} &= -\frac{c}{B} \frac{1}{r} \frac{\partial \tilde{\phi}}{\partial \theta} \\ r \frac{d\theta}{dt} &= v_{||} \frac{B_\theta}{B} + \frac{c}{B} \frac{\partial \tilde{\phi}}{\partial r} - \frac{c \bar{E}_r}{B} \\ R \frac{d\varphi}{dt} &= v_{||} \end{aligned} \quad (5)$$

Substituting (4) into (5), we obtain:

$$\frac{dr}{dt} = -\frac{c}{Br} \frac{\partial}{\partial \theta} \sum_{m,l,n} \phi_{m,l,n} [\cos(m\theta - l\varphi) \cos(n\omega_0 t) + \sin(m\theta - l\varphi) \sin(n\omega_0 t)] \quad (6)$$

Using two important properties of functions  $\sin$  and  $\cos$  which are:

$$\begin{aligned} \sum_{n=-\infty}^{+\infty} \sin(n\omega_0 t) &= 0 \quad \text{and} \\ \sum_{n=-\infty}^{+\infty} \cos(n\omega_0 t) &= 2\pi \sum \delta(\omega_0 t - 2\pi n) \end{aligned}$$

Then we have:

$$\frac{dr}{dt} = \frac{2\pi c}{Br} \sum_{m,l} m \phi_{m,l} \sin(m\theta - l\varphi) \delta(\omega_0 t - 2\pi n) \quad (7)$$

Hence this model spectrum gives impulsive jumps in  $r$  at

$$\text{time } t_n = \frac{2\pi n}{\omega_0}.$$

## II-2 Transformation into a mapping equation:

It is more useful to replace the equations of the guiding center particles motion with those of the

approach mapping. To achieve that, we introduce some new canonical variables.

We define these new angle-action variables  $(\chi, J)$  as:

$$J = \left( \frac{r}{a} \right)^2 \quad \text{and} \quad \chi = M\theta - L\varphi \quad (8)$$

$a$  is the minor radius of the torus. Also we suppose that only one perturbation mode  $(M, L)$  dominates in the equation of evolution of  $r$ . From equation (7) we have:

$$\frac{dJ}{dt} = \frac{2r}{a^2} \frac{dr}{dt} = \frac{4\pi c}{a^2 B} M \phi_{m,l} \sin(M\theta - L\varphi) \sum_n \delta(\omega_0 t - 2\pi n) \quad (9)$$

By integration over one jump at time  $t_n = \frac{2\pi n}{\omega_0}$ ,

equation (5) becomes in terms of  $\chi$ :

$$\frac{d\chi}{dt} = M \frac{B_\theta}{r.B} (v_{||} - \frac{c \bar{E}_r}{B_\theta}) - L \frac{v_{||}}{R} \quad (10)$$

Ignoring in first approximation of  $\bar{E}_r$ , the integration of the  $\chi$  and  $J$  differential equations as the function of time, then, we get their evolution equation:

$$J_{N+1} = J_N + \frac{4\pi c}{a^2 B_0} \frac{M \phi}{\omega_0} \sin(M\theta - L\varphi) \quad (11)$$

$$\chi_{N+1} = \chi_N + \frac{2\pi}{\omega_0} \frac{v_{||}}{q.R} (M - L.q) \quad (12)$$

## II-3 The standard nontwist mapping

(SNM): The important parameter which allows us to construct this model is the safety factor replaced

$$\text{here for convince by: } q(r) = \frac{r.B_\phi}{R.B_\theta}.$$

We suppose that this safety factor has a minimum local in the neighborhood of certain value  $r_m$ , it means that  $q_m = q(r_m)$ ;  $q'(r_m) = 0$ , since

$$\left. \frac{dq}{dJ} \right|_{r=r_m} = \left. \frac{dq}{dr} \right|_{r=r_m} \left. \frac{dr}{dJ} \right|_{r=r_m} = 0.$$

Then  $q$  possesses a minimum at  $J_m = J(r_m)$ .

We are interested in the motion of particles in the neighbourhood of  $r_m$ , and we do a Taylor development of  $q$  around  $J_m$ , we can write such development as:

$$q(J) = q(J_m) + \frac{q''_m}{2} (J - J_m)^2$$

While substituting this last equation in (10), we get:

$$\frac{d\chi}{dt} = \frac{v_{||}}{Rq_m} \left[ M - Lq_m - \frac{Mq_m^*}{2q_m} (J - J_m)^2 \right] \quad (13)$$

and after integration of the step of time  $\frac{1}{\Delta\omega}$  we obtain:

$$\chi_{N+1} = \chi_N + \frac{2\pi}{\omega_0} \frac{v_{||}}{Rq_m} \left[ \delta - \frac{Mq_m^*}{2q_m} (J_{N+1} - J_m)^2 \right] \quad (14)$$

Where  $\delta = M - Lq_m$

We introduce the dimensionless variables  $K$  and  $T$  such that:

$$K = \frac{\chi}{2\pi} ;$$

$$T = \left( \frac{Mq_m^*}{2q_m\delta} \right)^{1/2} (J - J_m) = k (J - J_m)$$

Hence, we can transform the system of mapping equation in the form of the SNM:

$$K_{N+1} = K_N + \frac{v_{||}\delta}{Rq_m\omega_0} (1 - T_{N+1}^2) = \chi_N + \alpha(1 - T_{N+1}^2)$$

$$T_{N+1} = T_N + \left( \frac{2\pi c M \phi}{a^2 B \omega_0} \right) \left( \frac{2Mq_m^*}{q_m\delta} \right)^{1/2} \sin(2\pi K_N) = T_N - \beta \sin(2\pi K_N) \quad (15)$$

Where

$$\alpha = \frac{v_{||}\delta}{Rq_m\omega_0} ; \quad \beta = \left( -\frac{2\pi c M \phi}{a^2 B \omega_0} \right) \left( \frac{2Mq_m^*}{q_m\delta} \right)^{1/2}$$

#### II-4 Global Mapping:

In order to introduce the effects of reversed magnetic shear and the radial electric field, we define the system of equation of global mapping that as follows<sup>1, 2, 5, 8-17</sup>:

$$J_{N+1} = J_N + \frac{4\pi c}{a^2 B_0} \frac{M\phi}{\omega_0} \sin(M\theta_N - L\varphi_N) \quad (16)$$

$$K_{N+1} = K_N + RK1(J_{N+1}) + RK2(J_{N+1}) \quad (17)$$

Where :

$$RK1(J) = \frac{v_{||}(J)}{\omega_0 q R} (M - Lq(J)) \quad (18)$$

$$RK2(J) = -\frac{cM}{\omega_0 a B_0} \frac{\bar{E}_r(J)}{\sqrt{J}} \quad (19)$$

$$v_{||}(J) = \sqrt{\frac{2}{m} (\zeta_t - e\Phi_0(J)) (1 - \lambda B_0)} \quad (20)$$

with :  $K = \frac{\chi}{2\pi}$ ,  $\zeta_t$  : the total initial energy,  $e$  : the

particle charge,  $\lambda = \frac{\mu}{\zeta_t}$  where  $\mu$  is the magnetic

moment and  $\Phi_0$  is the equilibrium potential as

$$\bar{E}_r(J) = -\frac{\partial\Phi_0}{\partial r} \Big|_{r=a\sqrt{J}}$$

#### II-5 Choice of the profiles of the factor of security:

The trajectories are already solved numerically according to this formulation of established mapping. However, we are going to give more importance to the control parameter  $q$ , and we are going to consider two configuration cases that are completely different.

We define two  $q$ - profiles of (**Figure 1**):

$$\spadesuit \text{ Normal: } q(r) = 1.99 + 1.94 \left( \frac{r}{a} \right)^2 \quad (21)$$

$$\spadesuit \text{ Reversed: } q(r) = 1.99 + 7.76 \left( \frac{r}{a} - 0.5 \right)^2 \quad (22)$$

The choice of the potential  $\Phi_0$  depends on the nature of the  $q$ - profile, therefore, in the normal case we

use  $\Phi_0(r) = -\Phi_0 \left( 1 - \left( \frac{r}{a} \right)^2 \right)$  and for the reversed

profile we take  $\Phi_0(r) = \Phi_0 \left( 1 - \left( 1 - \frac{2r}{a} \right)^2 \right)$ .

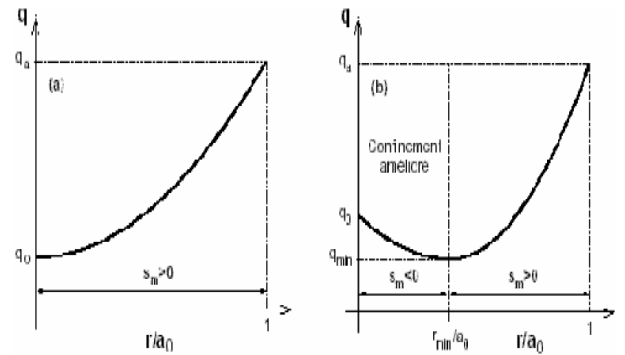


**Figure1.** Profile of the safety factor versus  $r/a$  for reversed (right hand) and normal (left hand) shear.

#### III-THE DIFFUSION OF THE PARTICLES<sup>1, 9-17</sup>:

To evaluate the plasma particles' diffusion through the magnetic surfaces within the tokamak reactors, we simulated in two cases the particulate diffusion coefficients. We expressed it under the most classic formula as follows:

$$D = \lim_{n \rightarrow \infty} \frac{\langle (r_n - r_0)^2 \rangle}{2t_n}$$

and we represented time evolution of the ratio of diffusion coefficient in reversed shear ( $D_r$ ) on diffusion coefficient in the normal case ( $D_n$ ) for deferent values of the perturbation (**Figure 4.**). Here  $t_n$  is a time step, We observe a large reduction of particles diffusion in the reversed case due to the transport barrier which have tendency to suppress the anomalous transport. The diffusion in the reversed case becomes lower than those in the normal case. And the formation of transport barrier which suppress turbulent transport may explain this reduction<sup>3</sup>.

#### IV- NUMERICAL SIMULATIONS & DISCUSSION:

In the next section, we investigate the map phase structure by calculating 1000 massive  $D^+$  trajectories with various initial conditions in configuration spaces for the reversed and normal shear cases of the safety factor.

We have used the TEXT and ITER Tokamak parameters<sup>1, 6, 8-17</sup>, and we simulate the parameters below. We observe that it is the same shape for the two tokamaks<sup>1, 9-17</sup> but for highest values of potential in ITER because for the smaller values of perturbation's potential, we could not observe any difference between the two profiles of the safety factor.

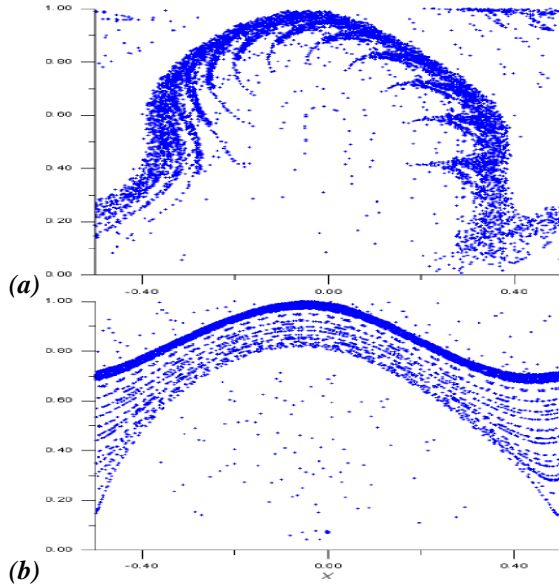


**Figure2.** Poincaré Section for 1000 particles in the  $(\chi, r/a)$  plane for the value  $1.5 \text{ eV}$  of the perturbation using TEXT parameters: (a) reversed shear; (b) normal shear.

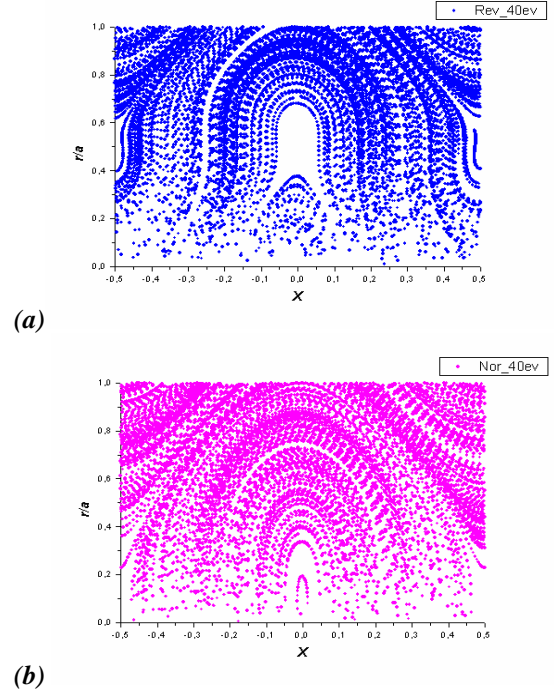


**Figure 2'.** Poincaré Section for 1000 particles in the  $(\chi, r/a)$  plane for the value  $40 \text{ eV}$  of the perturbation using ITER parameters: (a) reversed shear; (b) normal shear.

We observe in presence of the electrostatic perturbations and the normal profile of the safety coefficient  $q$ , the stochasticity of the trajectories increases and it is the principle reason for the particles' diffusion through the magnetic surfaces (**Figure 2.& 2'. (b)**).

While in the case of reversed shear, the principle result shows that the transport barrier<sup>4</sup> is near of surface that corresponds to the minimal value of  $q$  exists. This barrier plays an important role on the reduction of the transport and the diffusion of the particles, which drives to the improvement of the plasma confinement (**Figure 2. & 2'. (a)**).

The same conclusions is carried out in the case of the 3- dimensional simulation, we observe the same phenomena as those in the case of 2- dimensional simulation except that we do not see the formation of islands, and what we observe is a transition of the particles from the regions  $(r/a < 0.5)$  toward regions  $(r/a > 0.5)$ .

While increasing the amplitude of the perturbation, and in the reversed case (**Figure 3. (a)**) we observe that this transition drives to a transition of this barrier toward the outside regions of the tokamak  $(r/a \rightarrow 1)$  to prevent the diffusion of these particles. Whereas in the normal case (**Figure 3. (b)**), we observe that the majority of the particles escaped resulting in the total destruction of the magnetic surfaces of the confinement.

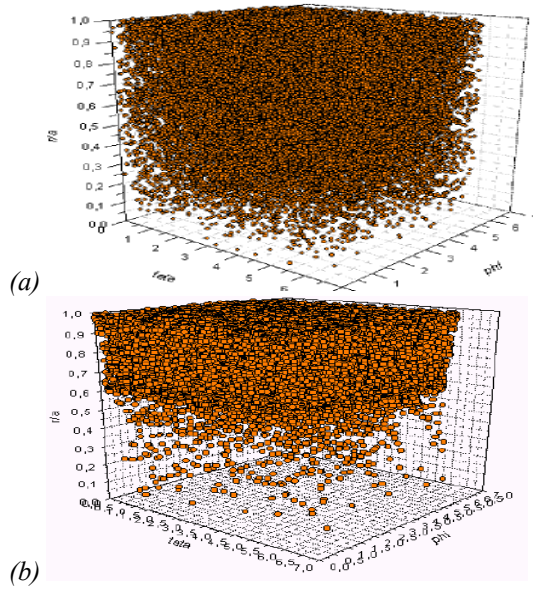


**Figure3.** Simulation of the trajectories of 1000 particles at 3- dimensional  $(\theta, \phi, r/a)$  for the value  $1.1$  eV of the perturbation: (a) reversed shear ; (b) normal shear.

According to the variation of the perturbation's potential ( $Pot$ ), we could observe tree different situations (Figure 4-a., 4-b. & 4-c.):

➤  $Pot \leq 1000$  eV: example  $100$  eV (Figure 4-a.)

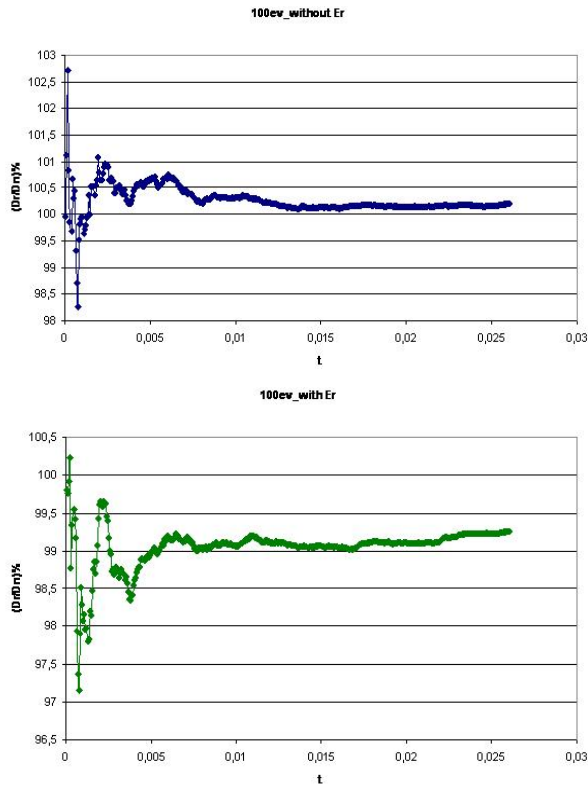


**Figure 4-a.** The ratio between the diffusion coefficient in reversed and normal shear as function of  $t_n$  in absence and in presence of radial electric field for  $Pot \leq 1000$  eV.

It is noticed that one has the same pace for the 2 cases: in absence and in the presence of the electric radial field<sup>7</sup> ( $E_r$ ), i.e. one witnesses a stability of the ratio  $(D_r/D_n)$  according to time, except that the values obtained in the 1<sup>st</sup> case are slightly more than those obtained in the 2<sup>nd</sup> case, this difference can vary from 1 to 6 %.

➤  $Pot = 1500$  eV (Figure 4-b.)

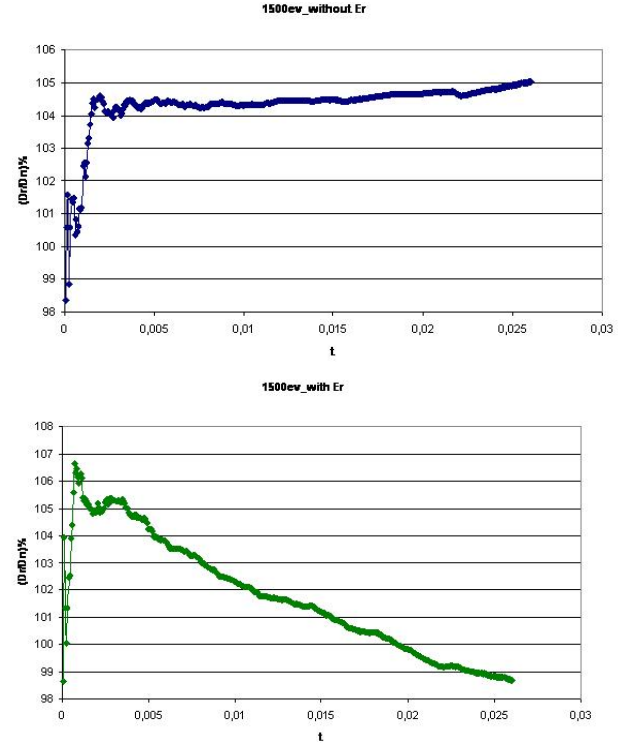


**Figure 4-b.** The ratio between the diffusion coefficient in reversed and normal shear as function of  $t_n$  in absence and in presence of radial electric field for  $Pot=1500$  eV.

In the 1<sup>st</sup> case, one observes that after certain rough fluctuations ( $< 0.002$  s), one attends a stability of the ratio  $(D_r/D_n)$ , while in 2<sup>nd</sup> case; one attends a fall of the curve which represents the evolution of this ratio according to time.

➤  $Pot = 2500$  eV (Figure 4-c.)

In the 1<sup>st</sup> case, one notices that there is a fall of the ratio  $(D_r/D_n)$  according to time, whereas in the 2<sup>nd</sup> case, one observes that there is an increase in this ratio what means that anomalous transport is supported.

#### IV- The influence of perturbation's modes on the particles diffusion:

In this paragraph we are going to study the influence of modes  $(m, n)$  on the instability and the diffusion in the ITER. Where the safety factor is:

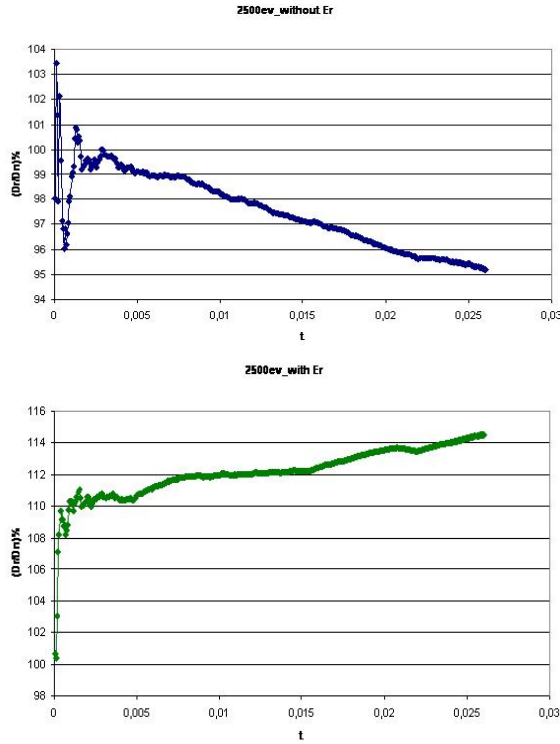


**Figure 4-c.** The ratio between the diffusion coefficient in reversed and normal shear as function of  $t_n$  in absence and in presence of radial electric field for  $Pot=2500eV$ .

$$q = \frac{\text{Nbr of torus in toroidal direction}(m)}{\text{Nbr of torus in poloidal direction}(n)} = \text{footprint (path) of the helix}$$

This factor is bound to the stability of plasma:  $q(0) > 1$  and  $q(R) > 2$  are necessary. The variation of  $q$  from a magnetic surface to the other creates a shear of plasma. This last can be decomposed then in dandruff that fits together the some without the other, to the manner of Russians toroidal dolls.

A particular case occurs when  $q$  is a rational (ratio of two integers): The field line does not describe the entire magnetic surface around which it surrounds. At every tower, the particle that turns around passes in the same place. This singularity leads to instabilities. In our studies, we plot the ratio of the diffusion coefficients in reversed and normal shear ( $D_r/D_n$ ):

In each perturbation's mode, while increasing the value of the perturbation's potential, the diffusion of particles increases progressively, it is confirmed by made it to have particles outside or inside the torus. While for the same value of  $q=2$  - for example - one observes that when  $m$  and  $n$  increase, the maximal perturbation's potential that one can reach decreases that wants to say one attends a divergence since small disruptions and the diffusion of particles increases. For a fixed  $n$ , if the value of  $m$  increases, the perturbation's potential decreases.

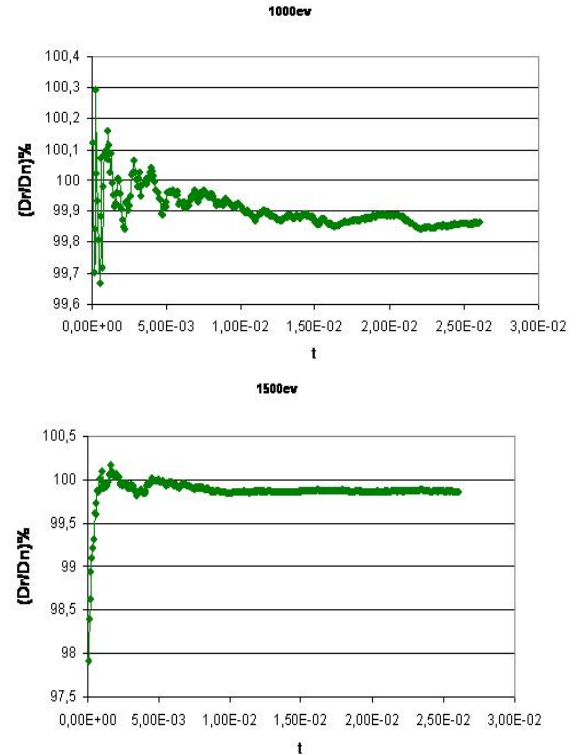
For all perturbation's modes, in the case of the perturbation's potential whose value is lower than  $300eV$ , after an increase of the ratio of diffusion coefficients value according to the time we attend at a stability of this ratio -after some fluctuations in the beginning- at the neighbourhood of 100%, except in the case of the mode  $(3, 1)$ , where we always observes an increase of this ratio. In the case of the potential of  $2000eV$ , while increasing the value of  $m$  and  $n$ , one sees that the value of the ratio stabilizes to a value slightly lower to the one gotten below ( $\approx 96 - 98\%$ ).

We have verified that the safety factor's variation between 1 and 3 did not affect the anomalous transport. The diffusion coefficient increases slowly as function of potential disruption and ends up stabilizing. For values of  $q \geq 3$ , we have showed that the diffusion coefficient increases fast for that we have an important anomalous transport.

## V- COMPARISON BETWEEN PARTICLES DIFFUSION ON ITER AND TEXT:

In this paragraph, we reproduce all simulations concerning the diffusion coefficient in two different tokamaks: ITER and TEXT, in order to be able to have an idea about the relationship between the size, the electrostatic perturbation and the diffusion coefficient in the normal and reversed shear for a given perturbation mode ( $M=12, L=6$ ).

(a)





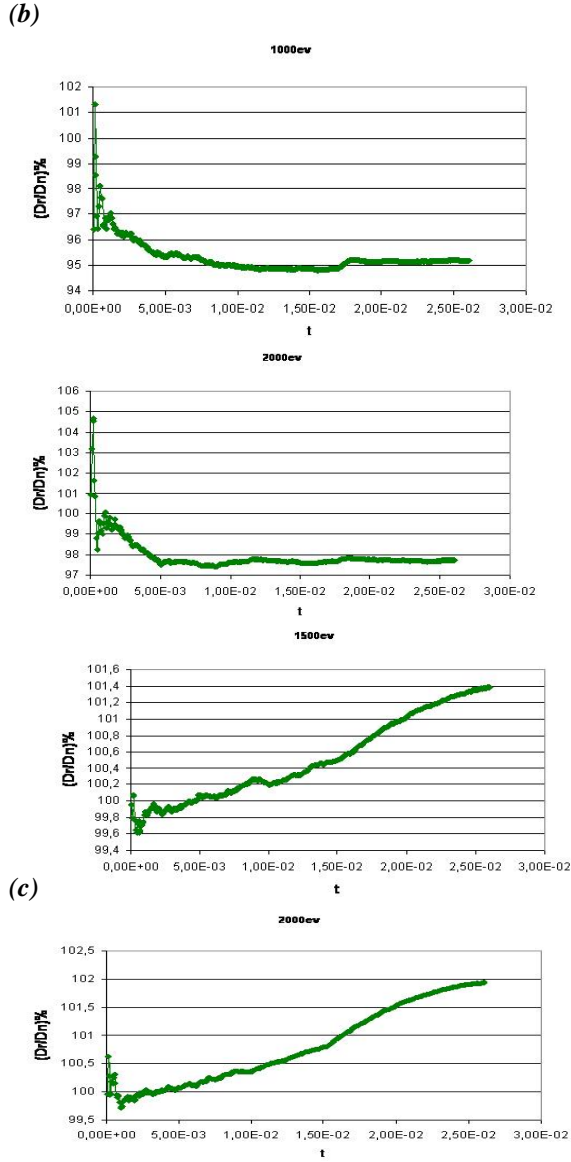


**Figure 5.** Particles diffusion for different perturbation's modes: (a) (5,3), (b) (50,25), (c) (3,1).

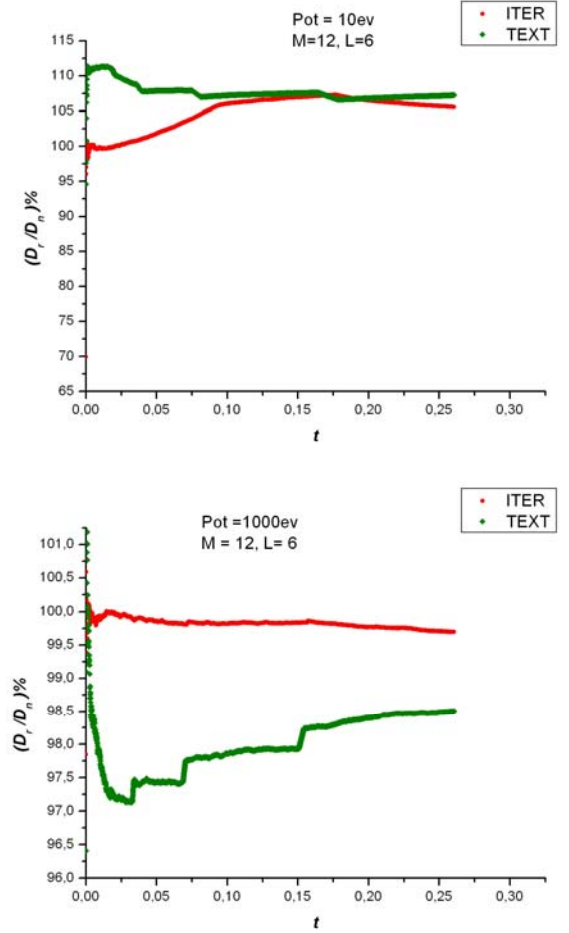
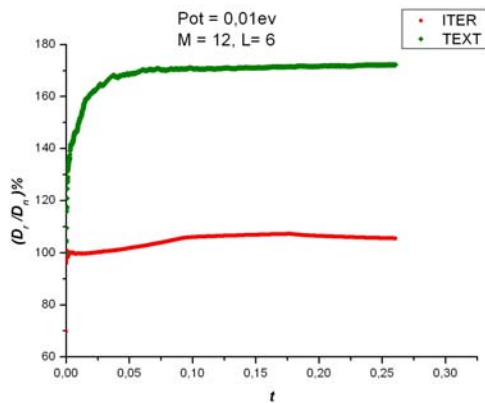


**Figure 6.** Comparison between particles diffusion in ITER and TEXT for different electrostatic perturbation.

We observe that for the weak perturbations the diffusion coefficient is higher in TEXT than in ITER which means that in the second tokamak there is no influence of perturbation at this stage. But since we increase the electrostatic perturbation, we see that this coefficient is increasing in ITER and decreasing in TEXT, and for strong perturbations, we observe that the diffusion coefficient is higher in ITER. For that, we could say that in a small tokamak, the diffusion is more important for weak perturbations while in a large one, the diffusion is more important for strong perturbations.

## VI. CONCLUSION:

The highest improvements in confinement and the greatest reduction in transport have occurred with transport barriers created in the plasma core while preventing its radial diffusion. The simulations show a clean reduction in the diffusion observed in the reversed magnetic shear profile. Therefore, the diffusion decreases, the confinement improves and the control of the fusion reactors to function in these modes permits the reduction of the anomalous

transport in the tokamaks. Again, the  $E \times B$  velocity shear is the dominant mechanism for the reduction in transport.

**Acknowledgement:** *The authors thank valuable discussions with Dr. X. Garbet. They are also grateful to him for his support, his opportunity to review these results and help anytime when they need.*

#### References:

- [1] W. Horton, H.B. Park, J.M. Kwon, D. Strozzi, P.J. Morrison, and D.I. Choi, 'Drift wave test particle transport in reserved shear profile', *Phys. Plasmas* Vol.5 No.11, 3910-3917 (November 1998)
- [2] O. Fisher, W.A. Cooper, L. Villard, 'Magnetic topology and guiding-center orbits in a reserved Tokamak shear'.
- [3] H. Takenaga et al., 'Determination of particle transport coefficients in reversed shear plasma Of JT- 60U'. *Plasma Phys. Control. Fusion* (1998).
- [4] Y. Kamada 'Observations on the formation of transport barriers', *Phys. plasma. Cont. Fusion* **42** (2000) A65-A80.
- [5] JLV Lewandowski and M. Persson *Plasma Phys. Cont. Fusion* **37**, N°11 (November 1995).
- [6] U. Samm 'Controlled thermonuclear fusion enters with ITER into a new era' (<http://www.jet.efda.org/documents/articles/articles.html>)
- [7] M.G. Bell, R.E. Bell, D.R. Ernst, B.P. LeBlanc, F.M. Levinton, E. Mazzucato, E.J. Synakowski, M.C. Zarnstorff, 'Radial Electric Fields and Transport Barrier Formation in TFTR', Princeton Plasma Physics Laboratory (REFP workshop / 000618-9)
- [8] T.P. Kiviniemi, T. Kurki-Suonio, S.K. Sipilä 'L-H Transport barrier formation: Self-Consistent simulation and comparaison with ASDEX Upgrade experiments', *Czechoslovak Journal of Physics*, Vol. 49 (1999), Suppl. S3.
- [9] M. El Mouden, D. Saifaoui, A. Dezairi, B. Zine, M. Eddahby, 'Transport barriers with magnetic shear in Tokamak', *Journal of Plasma Physics* (2006) Vol. 72, part 6, pp. 1-15.
- [10] M. ElMouden, D. Saifaoui, A. Dezairi, H. Imzi, 'Use Of Magnetic Shear For The Improvement Of Quality Of Confinement In The Plasma Of Tokamak', *FIZIKA A* 14 (2005) 4, 277 - 288
- [11] M. ElMouden, D. Saifaoui, A. Dezairi, A. Rouak, H. Imzi, 'The influences of the Magnetic Shear on the Improvement of the Quality of the Confinement in Plasma of Tokamak', 31<sup>st</sup> EPS Conference on Plasma Physics and Controlled Fusion. London (England), 28 June- 2 July 2004.
- [12] H.Imzi, D.Saifaoui, A.Dezairi, F.Miskane 'Contribution of reversed shear in reducing the anomalous transport', *Eur. Phys. J. AP* **17**, 45-52 (2002).
- [13] R. Tabet, D. Saifaoui, A. Dezairi, A. Rouak, *Eur. Phys. J. AP.* **4**, 329 (1998).
- [14] A. Oualyoudine, D. Saifaoui, A. Dezairi, A. Rouak, *J. Phys.* **7**, 1045(1997).
- [15] D.Saifaoui 'Contribution of reversed shear in reducing the anomalous transport' 28<sup>th</sup> EPS Conference on Controlled Fusion and Plasma Physics, Madeira Portugal 18-22 June 2001.
- [16] F.Miskane, A.Dezairi, D.Saifaoui, H.Imzi, H. Imrane, M. Benharraf 'Contribution of electrostatic and magnetic turbulence to anomalous transport in tokamak', *Eur. Phys. J. AP* **13**, 205-223 (2001).
- [17] M. ElMouden, D. Saifaoui, A. Dezairi, H. Imzi, 'The influences of Magnetic Shear on the Improvement of the Quality of Confinement in the Plasma of Tokamak'. *M. J. Condensed Matter*, Vol **5** N° 2; June 2004.